Mitteilungen der geodätischen Institute der TU Graz, Folge 33, pp 59 - 80

(54)

PRELIMINARY RADARGRAMMETRIC ASSESSMENT OF SEASAT-SAR IMAGES

*Franz Leberl**

Technical University, A-8010 Graz, Austria

ABSTRACT

Seasat Synthetic Aperture Radar (SAR) images were produced during the satellite mission between 4 July and 11 October of 1978. More than 1500 image strips were generated. Analysis of the data has been delayed due to the delay in converting the radar signals to imagery. Radargrammetric results are currently being generated, indicating that coordinate errors amount to about ± 100 m to ± 200 m if control points are used. This accuracy is limited by the problems of identifying control points. Radargrammetric applications of Seasat-SAR images are essentially in sea-ice drift studies. An early example is presented.

ZUSAMMENFASSUNG

Das Seasat Synthetische Apertur Radar (SAR) produzierte Radaraufnahmen zwischen dem 4. Juli und 11. Oktober 1978. Mehr als 1500 Bildstreifen wurden erzeugt, aber ihre Analyse geschieht mit großer zeitlicher Verzögerung wegen der langsamen Verarbeitung der Radarsignale in Bildform. Radargrammetrische Ergebnisse sind im Entstehen und ergeben vorläufig, daß Koordinatenfehler von ± 100 m und mehr trotz Vorgabe einer dichten Paßpunktbesetzung auftreten. Diese Genauigkeit ist durch die beschränkte Möglichkeit der Punktidentifizierung gegeben . Radargrammetrische Anwendungen der Seasat-SAR Bilder dienen der Beobachtung der Meereisdrift. Ein Beispiel wird beschrieben.

RESUME

Le radar latéral avec aperture synthétique (SAR) du satellite Seasat a produit des images à partir du 4e Juillet jusqu'à 1'11 ième Octobre 1978. Plusque 1500 images ont été produits, mais l'analyse est retardée, à cause du traitement optique et numérique qui est nécessaire pour la conversion des signaux radar en forme image. Les résultats radargrammétriques sont préliminaires; ils donnent une erreur de ± 100 m à ± 200 m avec des points d'appui. Les erreurs sont le résultat d'une identification limitéedes points. Les applications radargrammétriques des images Seasat-SAR concernent l'étude du mouvement de la glace sur mér. Le papier présente un example de cette application .

---

* This work is being carried out with Dr. Charles Elachi, Radar Science and Applications Group of the Jet Propulsion Laboratories, Pasadena U.S.A. and Dr. W. Campbell, Ice Dynamics Project, US Geological Survey, University of Puget Sound, Tacoma, U.S.A.

1. INTRODUCTION

Seasat was launched on 4 July 1978 as an oceanographic satellite with 5 sensors aboard (Figure 1): Scatterometer, five-frequency scanning microwave radiometer, altimeter, infrared radiometer and a synthetic aperture radar (SAR) with parameters as summarized in Table 1. The satellite was the first (civilian) one to carry an imaging radar system into a terrestrial orbit. Previous experiences with satellite radar only exist with the Apollo Lunar Sounder of the Apollo 17-Mission to the Moon (Phillips et al., 1973). There was hope that Seasat would do to radar what Landsat had done to MSS (Multi-Spectral Sensing): to stimulate worlwide research and interest in this technique. However, Seasat terminated its operation on 11 October 1978 due to an electrical short circuit. At the time of this event, 1502 successful orbits had generated masses of data. These were slow in

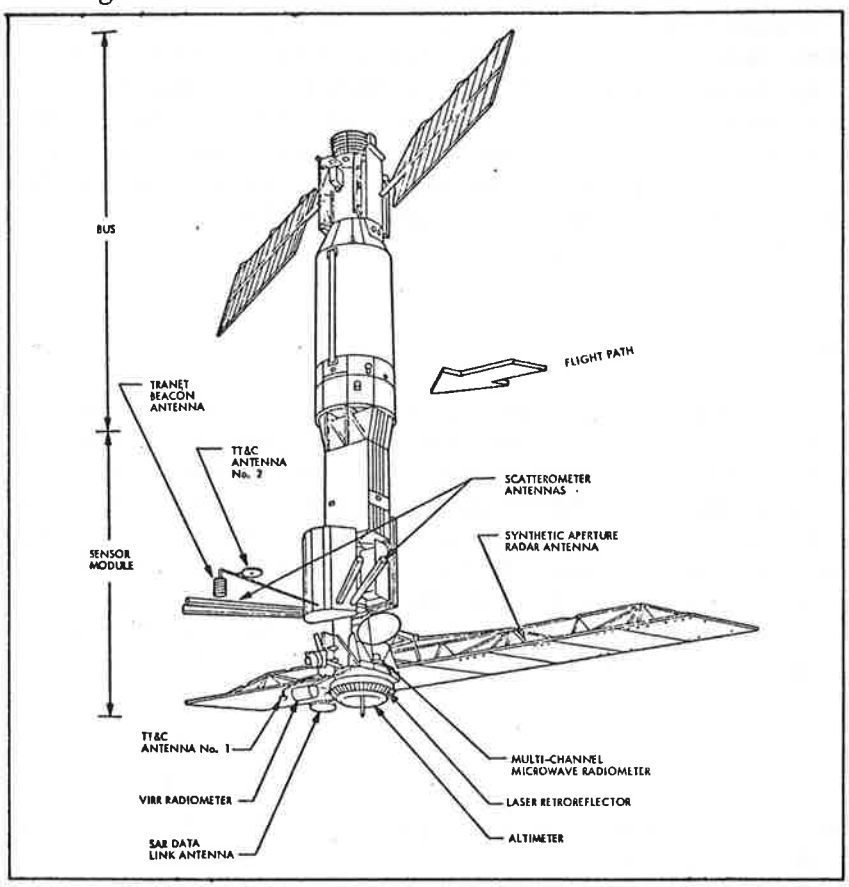

Figure 1: Sketch of Seasat satellite (from Teleki and Ramseier, 1978)

Mission duration	4 July - 11 October 1978
Orbit height	790 - 820 km
Orbit inclination	108 retrograde
Orbit period	100 min
Radar wave-length	25 cm, L-band
Radar look angle off nadir	17° to 23°
Swath width	100 km
Resolution	25 m nominal

Table 1: Seasat orbit and SAR-parameters

being processed through an optical correlator or through computer-image-formation (digital correlation). As a consequence the scientific results from image data analysis has been greatly delayed.

Seasat-SAR images are currently undergoing a radargrammetric analysis. An early paper was by Kratky (1979), however addressing only theoretical considerations and no actual imagery. This paper presents a progress report with some preliminary results from actual Seasat-SAR images. The analysis is motivated by the requirement of arctic sea-ice motion studies to be performed with Seasat-SAR images.

The paper will thus first review the Seasat-SAR-experiment and then describe test imagery used for the radargrammetric analysis. This preliminary analysis is based on an evaluation of image deformation using simple transformations of the image into the map coordinate system. It becomes evident that point identification can cause severe limitations of radargrammetric accuracy. A set of examples will be presented to highlight these limitations. Finally the measurement of sea-ice motion is demonstrated to illustrate the applicability of Seasat-SAR to this task.

3. THE SEASAT-SAR EXPERIMENT

The imaging radar was part of Seasat's sensor package to provide an all weather capability for ocean monitoring. The radar produced images at look-angles off-nadir of 17° - 22° (compare Figure 2). According to Teleki and Ramseier (1978) the following main goals were pursued:

- study ocean wave patterns in deep ocean, in the continental shelf and in costal regions;
- derive wave spectra;
- obtain information on land-water interaction in coastal areas;
- study sea- and fresh-water and snow cover;
- obtain experiences in studying land surfaces with radar (roughness, materials, landforms, vegetation, environmental data).

Satellite sensing has the great advantage over airborne sensing that repeated observations of changing phenomena -- this is often described as "monitoring"--- are feasible with a minimum of variable cost. But in addition, there were expectations that satellite radar has the following advantage over airborne radar (Leberl, 1978 a):

- large swath (100 km) with small variation of angle of illumination;
- reduced geometric deformation due to small variation of look-angle;
- higher accuracy due to stable satellite orbits;
- comparatively small variable cost for repeated coverage of quickly changing phenomena.

In the discussion of the results it will become apparent that in the particular example of Seasat-SAR data processed in this analysis, the expectations were only partly met.

From Table 1 and its Seasat-mission parameters one can conclude that the satellite was capable of imaging any point on the Earth's surface. No recording of data was however possible due to the high data rates. In fact, only those

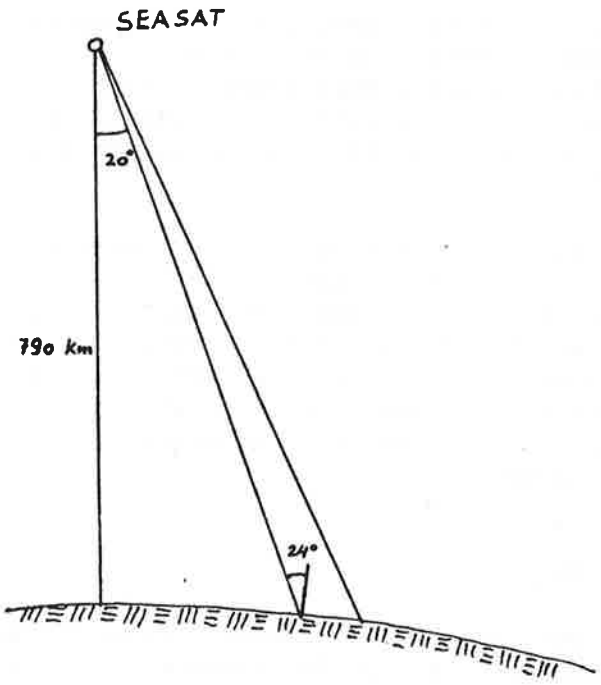

Figure 2: Imaging arrangement for Seasat-SAR

parts could thus be imaged with SAR that were within reach of a ground receiving station. There were five: Fairbanks, Alaska; Shoe Cove, New Foundland; Oakhanger, England; Goldstone, Calif., Merrit Island, Florida.

The satellite had enough power to image for a period of about 10 minutes per orbit. At a ground speed of 7 km/second, the images would thus cover a swath of about 4000 km length.

With a nominal ground resolution a of a = 25 km, and film recording with a resolution of about n = 10 linepairs per millimeter, a recording scale 1: M of 1:700 000 would be required, since (compare Leberl, 1978 b):

$$M = a * n * 2800$$

Seasat data are recorded at a scale of about 1:500 000 to about 1: 600 000. Due to the use of cathode ray tubes (CRT's) for optical generation of SAR images, there were limitations to the number of pixels to be presented across the face of the CRT. To resolve this limitation, the entire swath of 100 km width covered on the ground was imaged onto 3 or 4 strips of film in such a way that small overlaps exist between strips. A typical set of such image sections is shown in Figure 3 a. The digitally generated images were directly put onto a single strip of film as seen from Figure 3 b.

Optical versus digital processing is still an item of intense discussion among investigators and users of SAR imagery. As apposed to real-aperture radar, SAR-images are produced in two sequential steps (for a more detailed discussion see Harger, 1970) first the raw radar echoes are used to generate a holographic record, comparable to an image line. The sum of many such records or "signal histories" must then be converted to an image usable by the interpreter. Up to very recently, the conversion has been optically, generating first a photographic record of the signal histories, and then converting them,

Figure 3 a:
Seasat-SAR image of Los Angeles, Orbit 351, (21 July 1978), digital correlation.

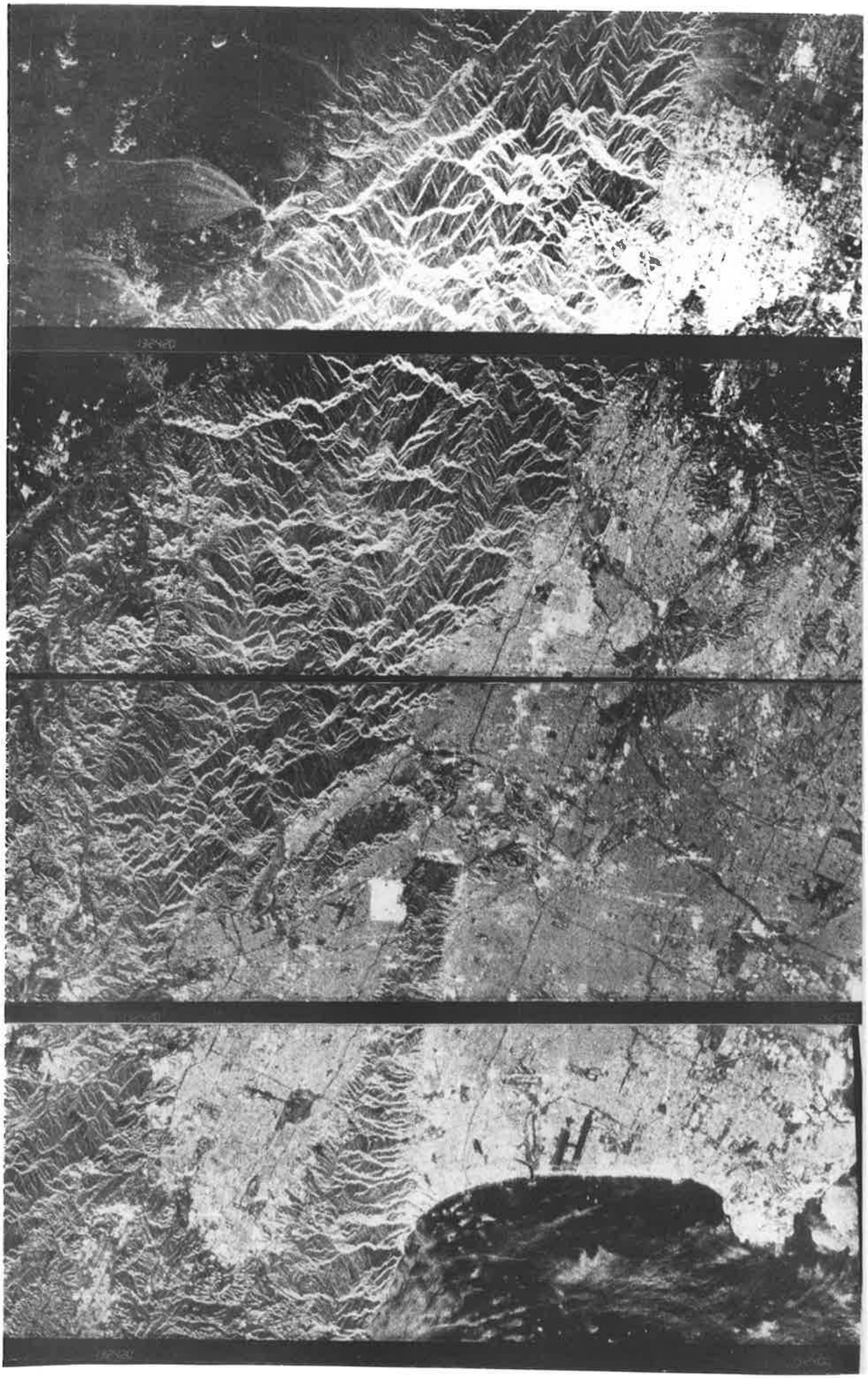

Figure 3 b: Seasat-SAR image of Los Angeles, orbit 351, taken on 21 July 1978 with optical correlation.

using coherent illumination (laser) and a set of spherical and cylindrical lenses (compare Leberl,1978 a). In the wake of the Seasat-project, operational alternatives developed that employ digitized signal histories and a computer to generate the final map film. Currently there are two such systems available: at the Jet Propulsion Laboratory (JPL), Pasadena, USA and at Macdonald, Detwiler & Assoc.; Richmond, Canada. In fact, digital radar correlation and processing may owe its decisive breakthrough to Seasat-SAR.

It is fairly obvious from Figures 3a and b that digitally processed SAR-images have a resolution superior to those processed optically. This becomes even more obvious in the enlargement of a section of Figures 3 a and 3 b, presented here as Figure 4 together with a section of a street map of the area.

3. TEST IMAGERY AND MEASUREMENTS

Initial measurements were made with a set of images over Salton Sea in California, USA, one of the first data that became available. The optically correlated image was from orbit 150, taken on day 188 (7 July 1978) at 12:17 hours. The digitally correlated image is from orbit 1140, taken 14 September 1978 at 17:00 hours.

Presentation of both images is in slant range (see Figure 5 a, b). The optically correlated image consists of a total of 3 strips that overlap for 2.5 km. Only two are presented. In the south a distinct linear demarkation represents the U.S.-Mexican border. Change in housing arrangements is responsible for the different radar echos to both sides of the border.

In addition to the images, also maps are available at scales 1:250 000, 1: 64 500 and 1:24 000. The most recent one is the 1: 250 000, from 1969; the larger scale maps are from 1957 and often so outdated that orientation is difficult in radar images.

Digitally correlated images from JPL do not have any range or time marks at all, optically correlated images in principle have such marks, but not in all cases. The images from orbit 150 did not carry any marks. It is thus impossible to derive ground coordinates from this Seasat data alone. However, the main interest initially is on the internal accuracy of the SAR-images and the error with which one feature can be located with respect to others. Therefore the use of ground control is here acceptable.

In order to obtain some early indication about the accuracy of locating points with Seasat alone, the second test set with an image of Los Angeles was employed as presented in Figures 3 and 4. That image did have tick marks.

optical

digital

map

Figure 4: Enlargement of a detail from Figure 3 with steet map at scale 1:50 000 (intersection of Santa Monica and Harbour Freeways and University of Southern California). 1 km

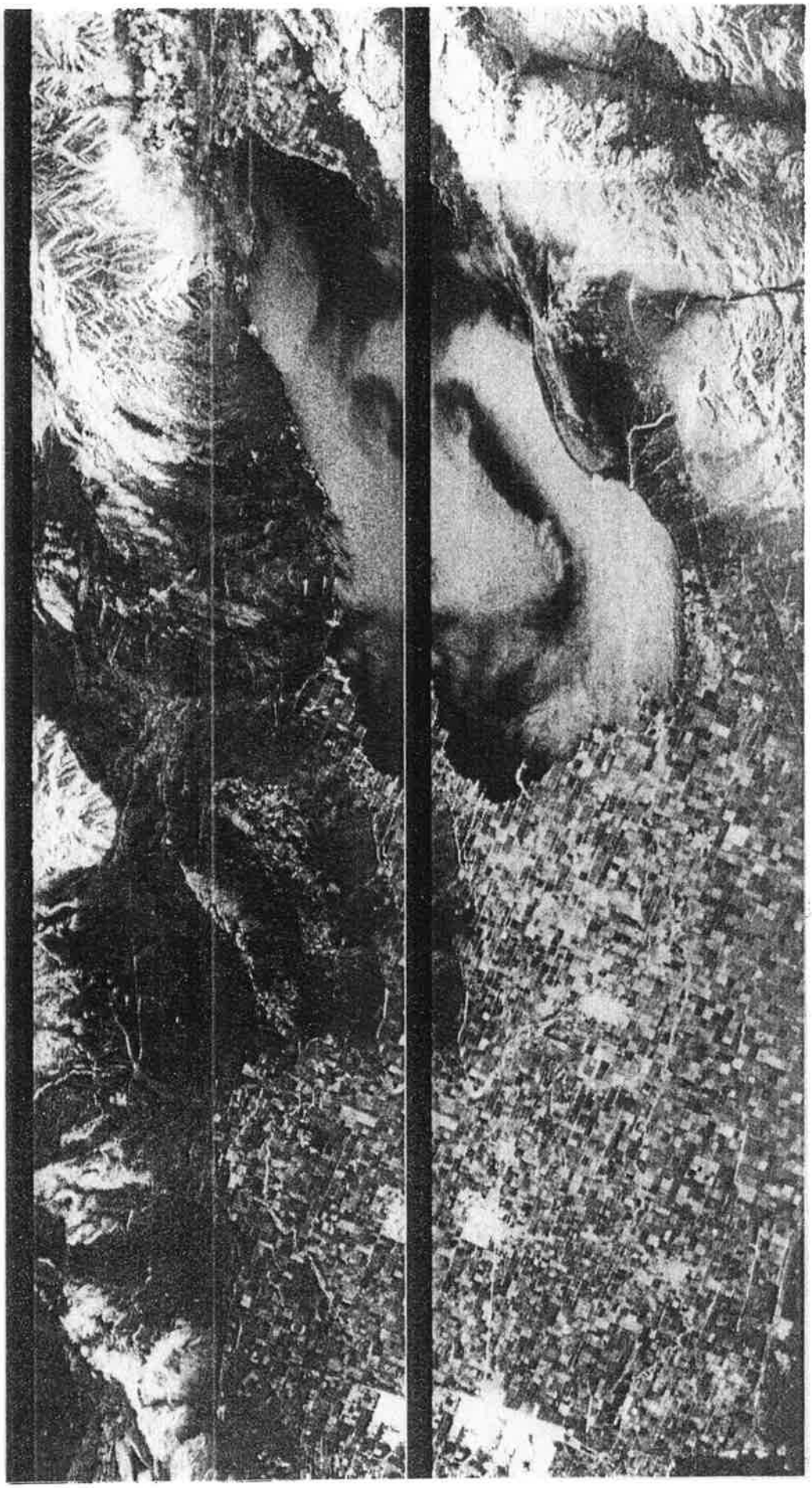

Figure 5 a: Seasat-SAR Image of Salton Sea and Imperial Valley California with optical correlation; orbit 150 (two of a total of 3 strips).

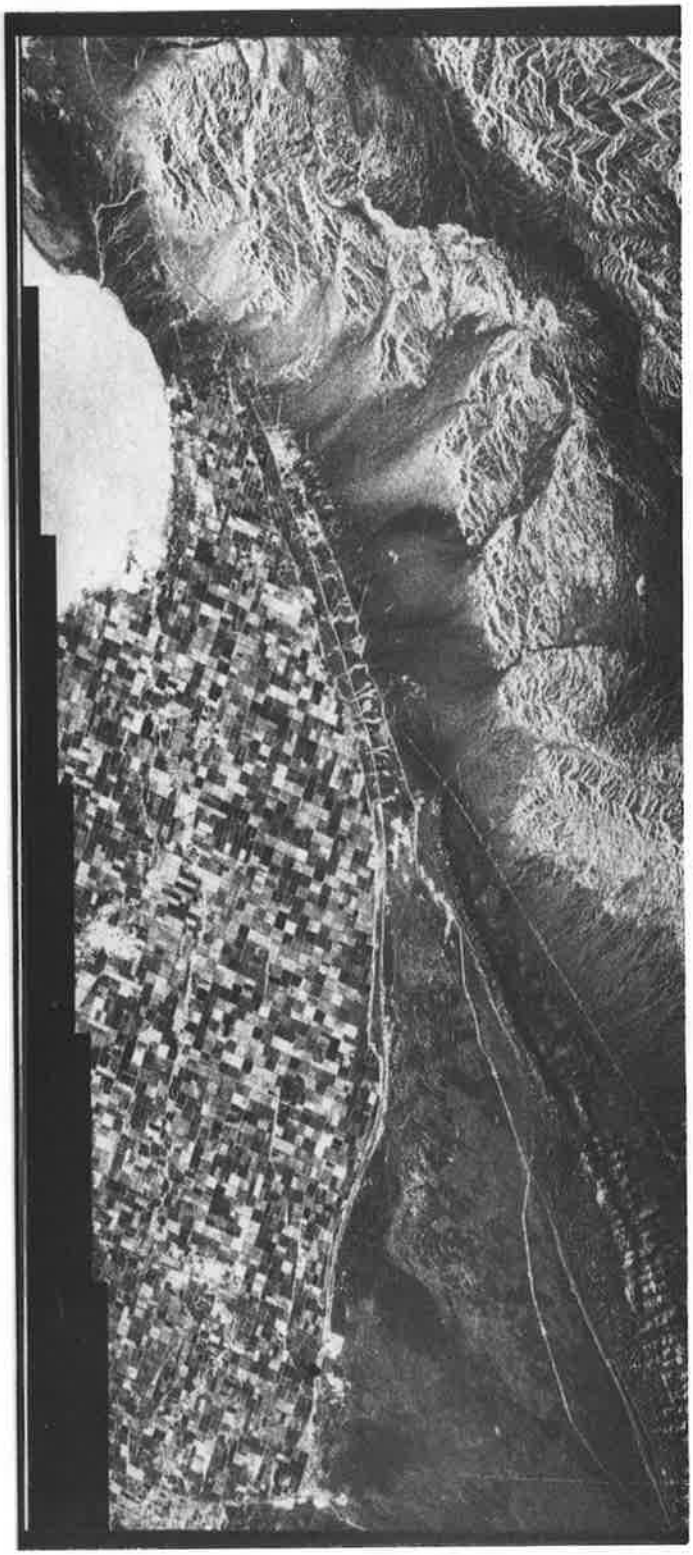

Figure 5 b: Seasat-SAR image of Salton Sea and Imperial Valley, California, with digital correlation, orbit 1140.

On the images, both the optical and the digital one, ground points were identified, that are also available on the map. The distribution of ground points for the Salton Sea area is shown in Figure 6. Co-ordinates were scaled off the map with an accuracy of better than ± 0.5 mm or 12.5 m on the ground. Image coordinates were measured in a photogrammetric mono-computer with superior recording accuracy.

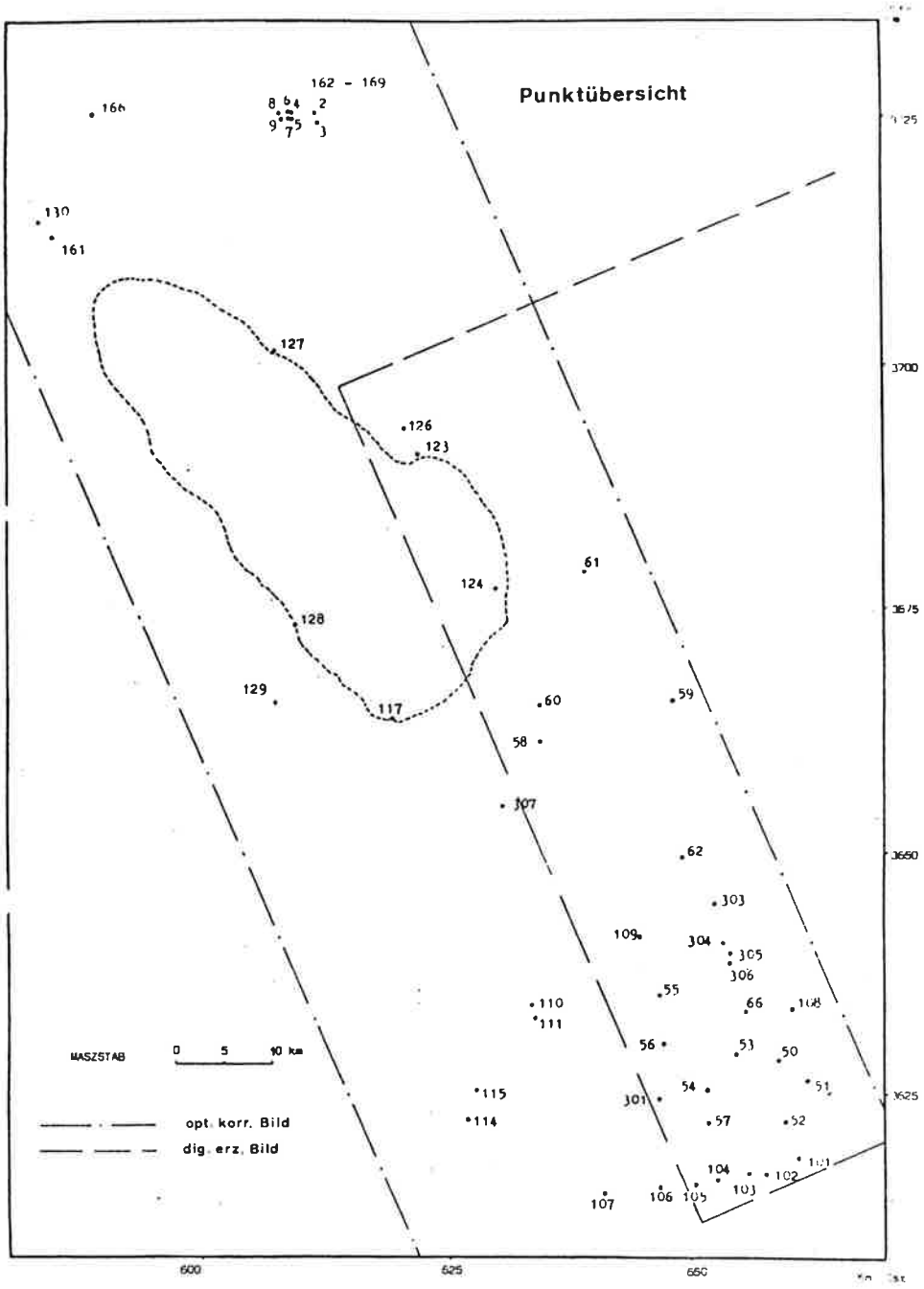

Figure 6: Distribution of ground control points for the deformation analysis in Salton Sea images.

4. IMAGE DEFROMATION

Radar image geometry is fairly well understood and documented. A review of radar mapping work was presented by Leberl (1976). However, rather than employing the full complexity of rigorous radargrammetric models, it is appropriate to study, in an initial phase, only image errors viewing the SAR-image as a map substitute. This initial analysis can thus be based on simple transformations between image and map.

Table 2 presents the root mean square discrepancies between the radar images and maps. The following transformations were used:

Meter	optically correlated		digitally correlated	
	m_x	m_y	m_x	m_y
Linear conformal	300	273	502	574
five-parameters	292	243	535	222
six parameters	284	241	119	198
eight parameters	220	349	155	188
moving average	120	113	170	208

Table 2: Seasat-SAR image deformations (in meters) after transformation of image points into the map using ground control points and

linear conformal transformation:

$$E = a + bx + cy, \qquad (1)$$
$$N = d - cx + by;$$

linear 5-parameter transformation:

$$E = a + bc + cy + ex \qquad (2)$$
$$N = d - cx + by;$$

linear 6-parameter transformation:

$$E = a + bx + cy, \qquad (3)$$
$$N = d + ex + fy;$$

bi-linear transformation:

$$E = a + bx + cy + gxy \qquad (4)$$
$$N = d + ex + fy + hxy;$$

and a moving average interpolative method, where the point to be interpolated is considered a "new point" so that its interpolated coordinates can be evaluated against map values.

In theses equations, E, N denote easting and northing coordinates of points in a UTM system x,y denote image coordinates. The "moving average method" is a general purpose, point-wise local interpolation algorithm as described for example by Leberl (1975).

Clearly there are significant affine deformations in the data, since results improve when an affine transformation is employed (equ. 3) rather than a conformal one (equ. 1). Differences of scale amount to about % The moving average method did not produce improved results -- the method requires a regular distribution of points and produces degenerating results when used for extrapolation as is the case here for isolated control points.

5. IDENTIFICATION ACCURACY

The surprising result is the lack of significant geometric accuracy differences between optically and digitally correlated images. While they appear greatly different in quality to the observer, their accuracies seem to be nearly equal. Apparently the points that can be identified in both, optical and digital images alike can equally well be measured, while there is no doubt that many more points can be identified on the digital than on the optical image.

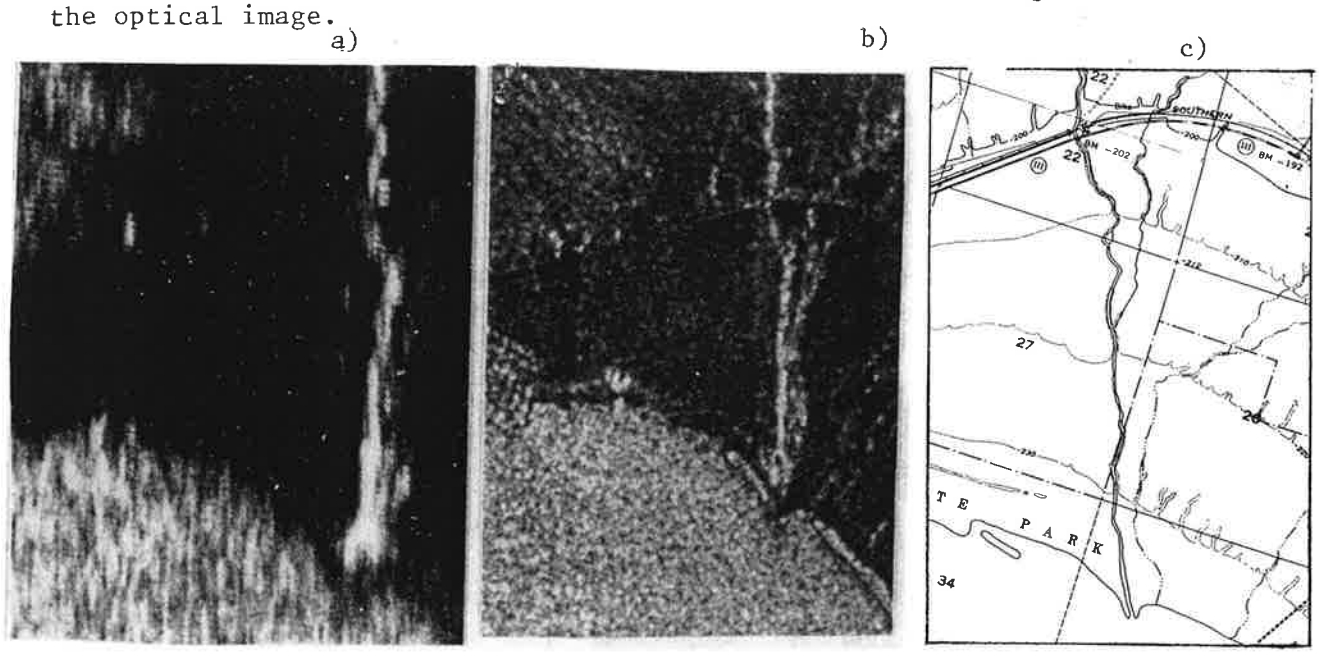

Figure 7: River flowing into Salton Sea and railroad bridge, with (a) optical correlation, (b) digital correlation, (c) map of scale 1:24 000.

Figures 4 a,b,c presented one example of an urban street pattern and may give an indication of the difficulty to orient oneself on Seasat-SAR images. Other examples are shown in Figures 7 through 10. Figure 7 demonstrates that a fairly large river flowing into the Salton Sea can easily be identified, but the exact location of the river mound, and of an intersection between a railroad line and the river, are less distinctly identifiable.

a) b)

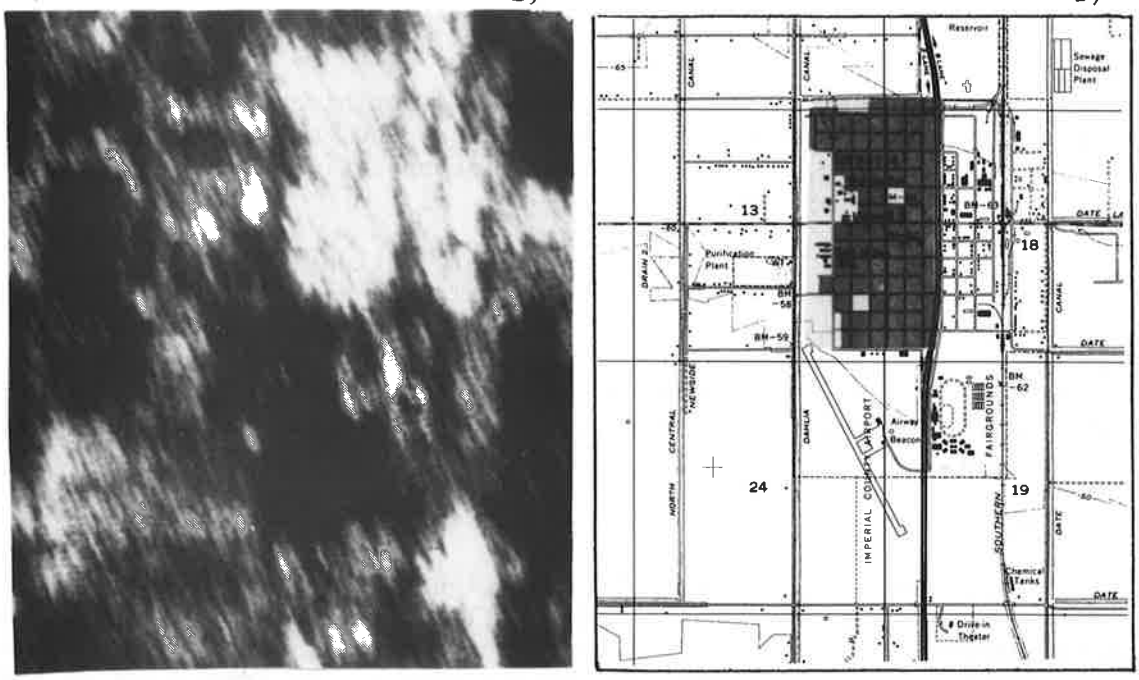

Figure 8: The city of Imperial with its airport in the (a) optical, (b) the map 1:24 000. Note the railroad track in the lower right part of the image as it shows up strongly and disappears after a turn away from the satellite orbit track.

Figure 8 presents an airport of the city of Imperial, California. The airport is large enough to be imaged clearly. However, the concrete runway and surrounding level grass fields merge to an indistinct dark image area -- the airport runway is therefore not identifiable. The image also shows a railroad line that bends, coming from the south, when it approaches the airport. In the southern part of the image, the railroad is parallel to the orbit of Seasat and due to strong specular reflections the railroad is well visible. After the slight bend, the line disappears completely.

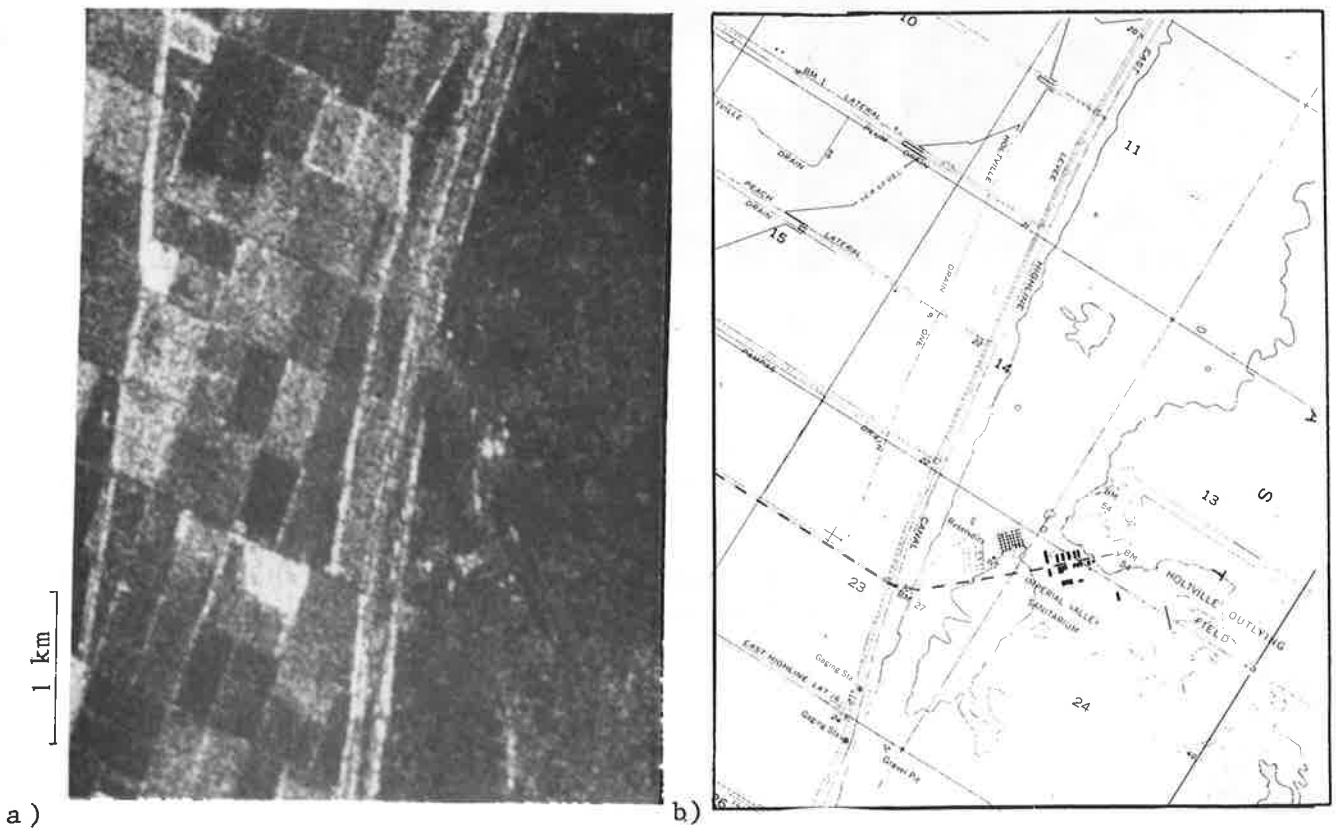

Figure 9: Intersection of road and canal (a) digital image (b) map 1: 24 000.

Figure 9 shows the intersection of a road and canal on the digital image and on the map, illustrating the difficulty to identify even the largest man-made structures unambiguously. The airstrips shown here in the map are this time also well identifiable on the radar, presumably due to surface roughness differences on the runway and surrounding fields.

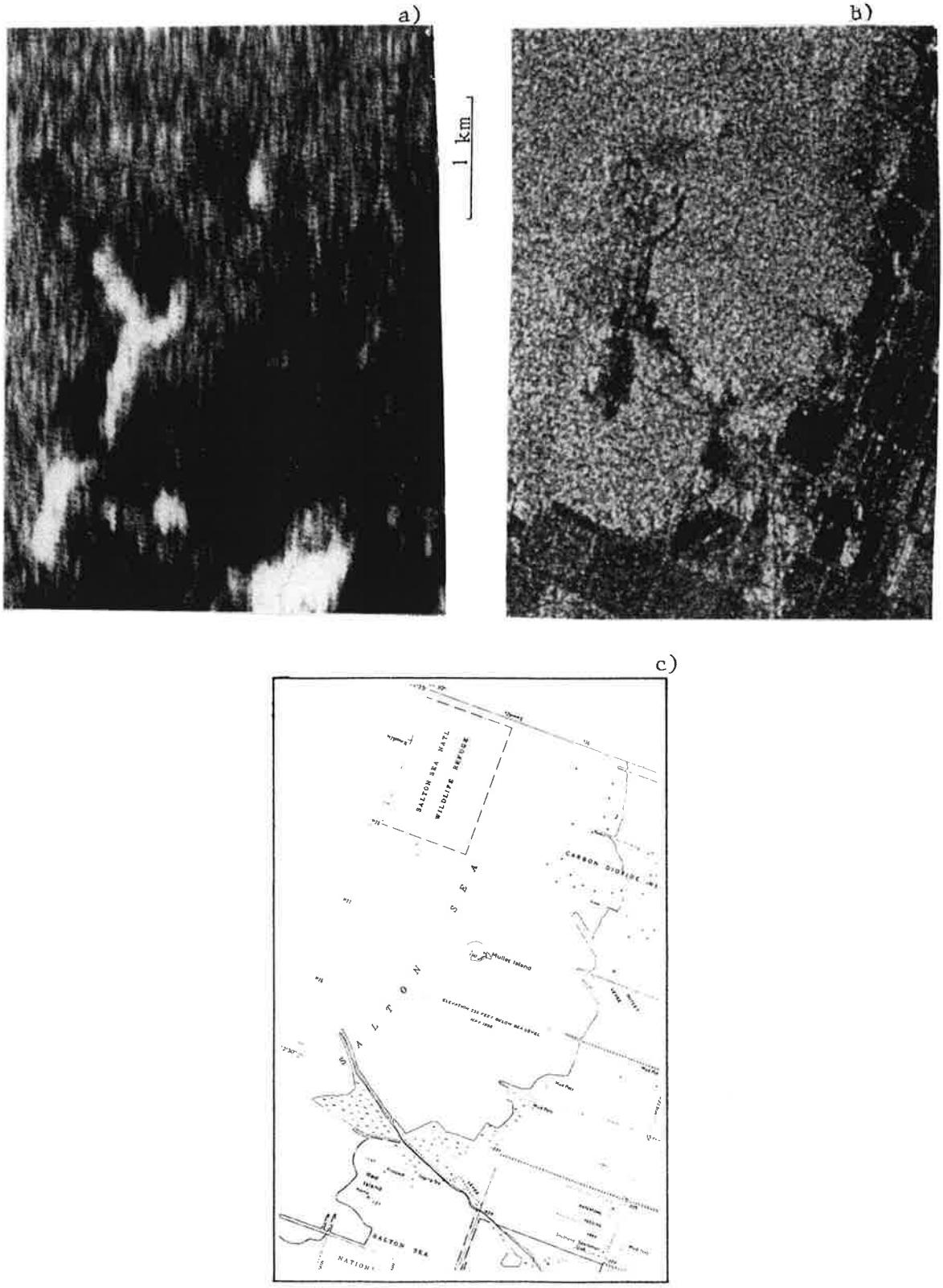

Figure 10: Island and delta in the Salton Sea, on (a) optical, (b) digital image and (c) on map 1:24 000.

Figure 10 contains the shore line of Salton Sea, an island and a river delta on the optical and digital image, and on the map. Due to the wind induced water waves on the lake, the radar echos reflect back to the antenna and create bright images of the water surface. This is quite different from airborne radar operated at much larger look-angles off-nadir, where water always is black and creates no radar returns to the antenna. The steep look-angle of Seasat, however, causes the land-water interface to become rather fuzzy and hard to identify, to the point where the island can hardly be found on the digital image (note that the optical and digital image were taken at different times!).

Figure 10 also illustrates another difficulty: the map shows a delta as it was in 1957. The radar shows the delta from 1978. Apparently there was a change, with the delta going into direction of the island. The problem of on outdated map thus adds to the difficulties already hampering image identification. Identi fication of the shoreline is illustrated in Figure 11.

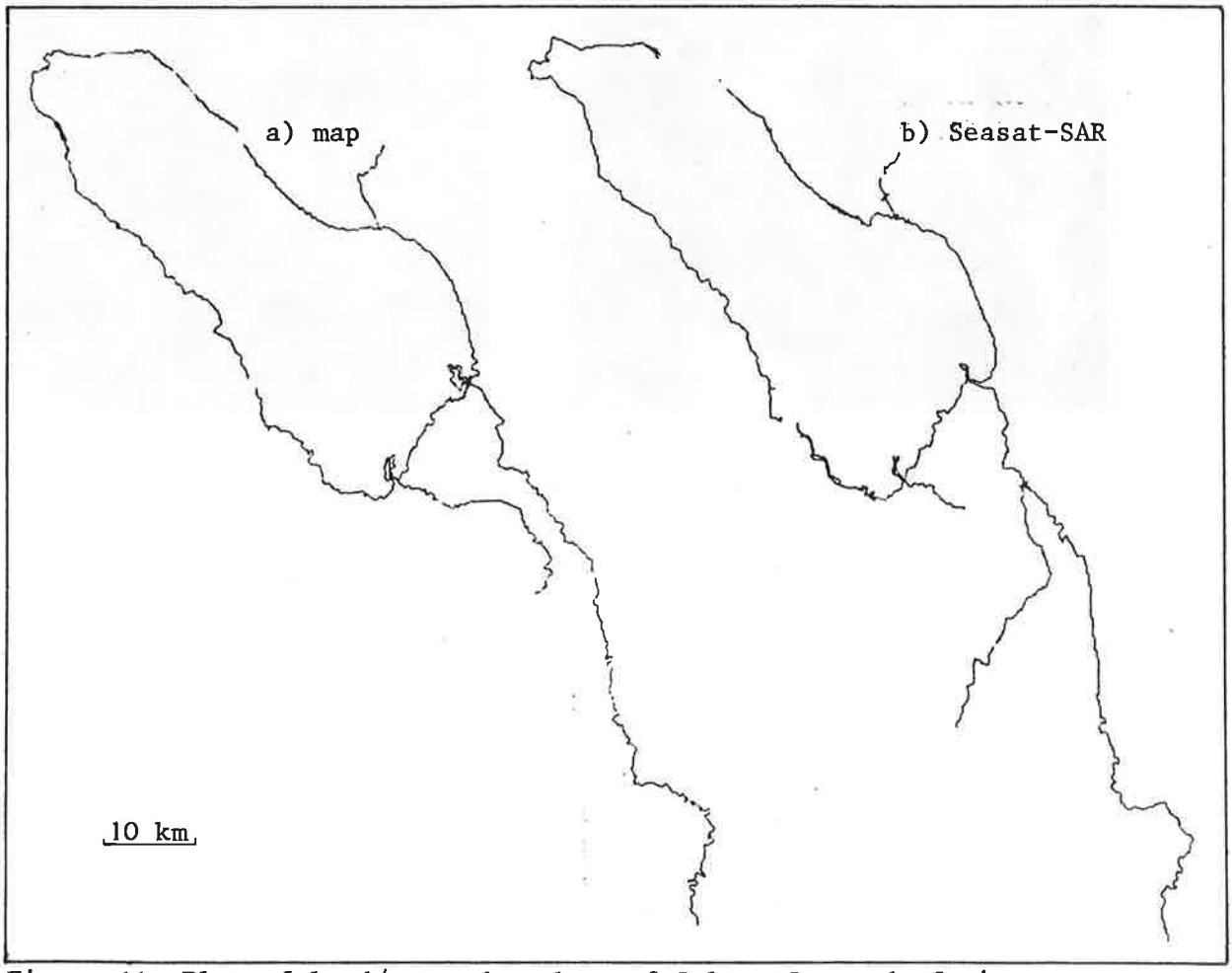

Figure 11: Plot of land/water boundary of Salton Sea and of rivers, as plotted from (a) the map 1:250 000 and (b) the Seasat SAR optical correlation.

The fact that the optical and digital images were taken at different times also permits to point out an interesting fact: in many instances the gray tones are totally changed from 7 July (optical image) to 14 September (digital image). As seen from Figure 12 the same area can change so completely that identification of common points becomes nearly impossible, inspite of a dense arrangement of canals and roads, man-made features that are generally so well identi-

fiable on aircraft radar data of flat areas.

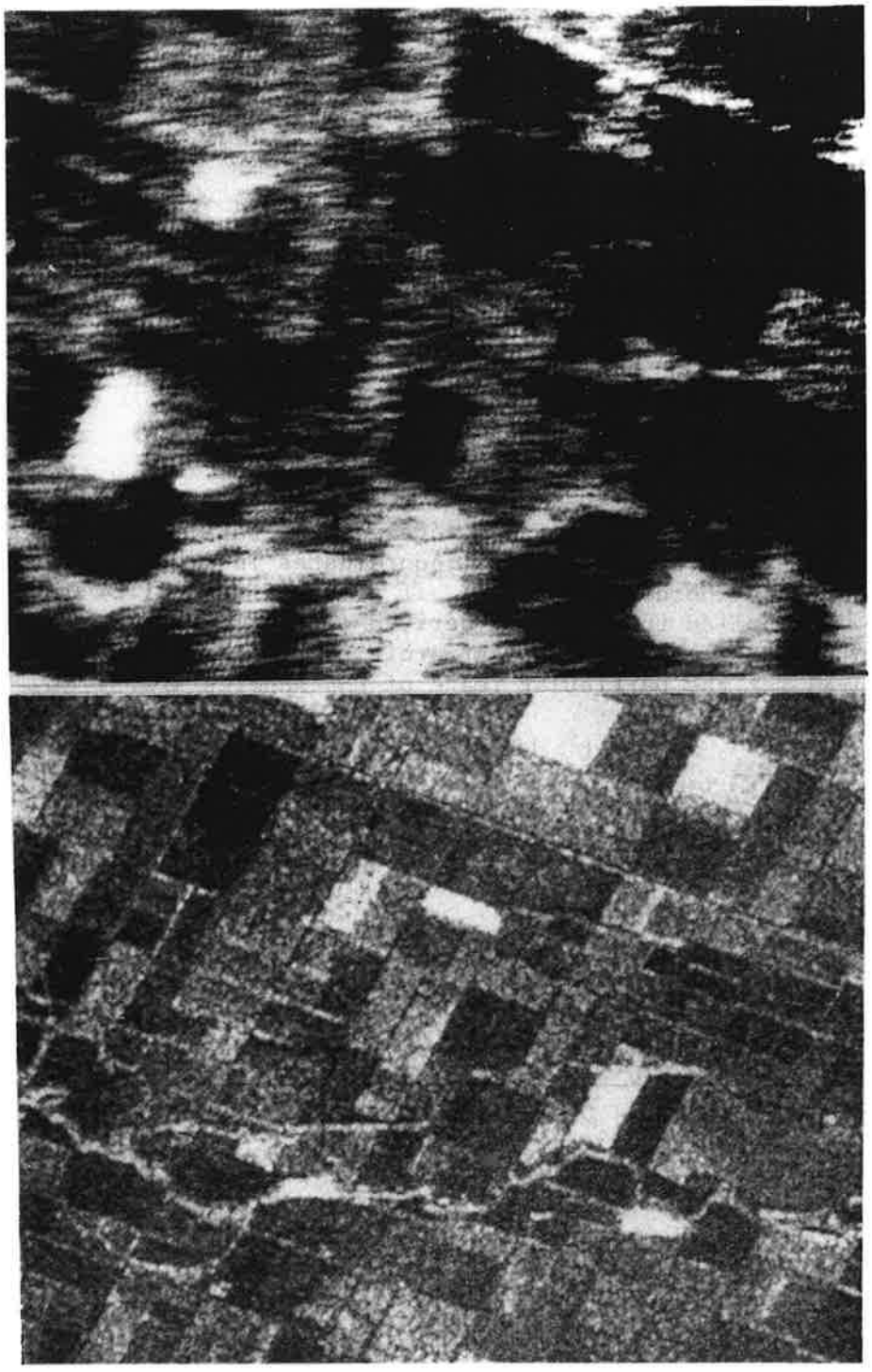

a)

b)

Figure 12: Optically correlated image (a) and digital one (b) as taken 2 months apart of an agricultural scene. Note differences in gray tones in the agricultural pattern.

Acutal errors of identification can be evaluated when many closely spaced points are measured on the images and a map transformed into another. Residuals are the result of identification errors rather than of remaining image deformation, since one deals with a very small area only. Table 3 presents the result of evaluating identification errors with 21 points distributed over a comparatively small area of cm^2 in the image

or km^2 on the ground.

Meter	optically correlated		digital correlated	
	m_x	m_y	m_x	m_y
all points (21)	202	207	300	357
good points (15)	57	48	47	72

Table 3: Coordinate errors due to limited identification of points.

6. LOCATING POINTS WITH SEASAT-SAR

Using the optical image of Los Angeles, several points were transformed from the x,y-image system to ϕ, λ, coordinates in a geographical system and compared to coordinates scaled off a map at scale 1:24 000. No correction was applied to the radar-derived ϕ,λ values, which were solely based on the tick marks and Seasat orbit values. The resulting errors encountered for the particular image of Los Angeles are:[1)]

$$\delta_\phi = 1^\circ\ 10' \quad ; \quad \delta_\lambda = 0^\circ\ 40'$$

7. SEA-ICE MOTION

7.1. Data

Repeated Seasat-SAR passes are available with images covering the same area in the Arctic and suitable for the measurement of sea-ice drift. For a first demonstration, 5 SAR-passes have been selected as described in Table 4; these images begin over Banks Island, Canada and stretch into the

Revolution	Equator Crossing	Day of year	Time on	Time off	Highest latitude
1038	297°77	250	14:02:12	14:05:52	71°66
1081	297°84	253	14:16:30	14:18:30	71°78
1296	297°85	268	15:19:10	15:23:10	71°97
1339	297°84	271	15:32:53	15:34:53	71°71
1382	297°82	274	15:45:36	15:47:36	71°80

Table 4: Seasat SAR images (passes) for Sea-ice demonstration, Beaufort Sea.

Arctic and on to nearly reach northern Siberia, thus crossing the entire Beaufort Sea.

The entire strips are several meters long -- at scale 1:500 000, an

1) The cause for these excessive errors has not been identified at this time.

image covering 4000 km extends over 8 m. It is thus reasonable to initially only work with part of the whole image. Figure 13 thus shows parts of two of the 5 passes, beginning at Banks Island and going on for about 400 km. Ice floes A and B are marked in both passes. The images do carry time marks for each second of time and Seasat orbit data are also available for each second along the orbit.

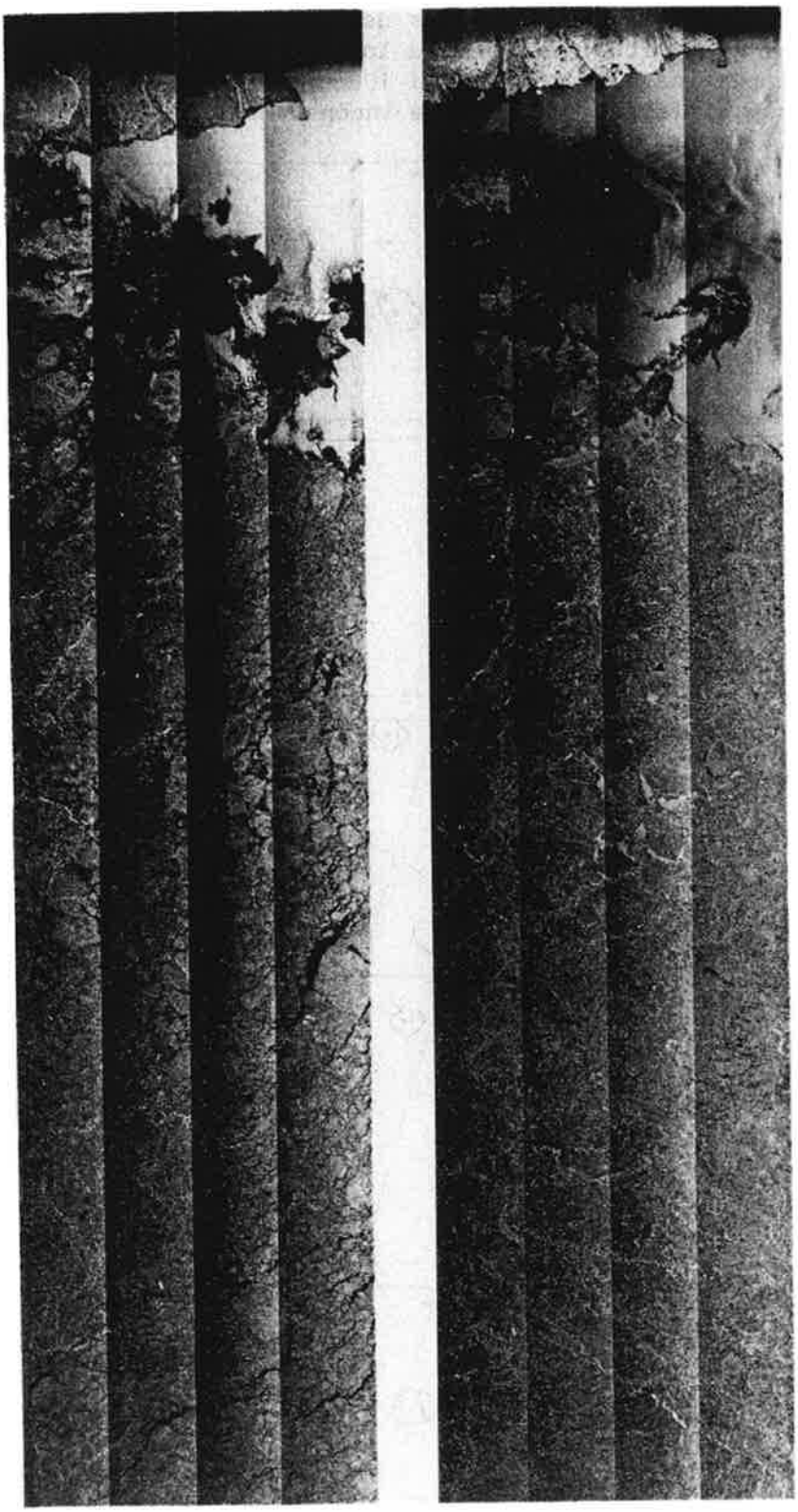

25km

Figure 13:Arctic Sea-ice in Beaufort Sea as imaged by Seasat-SAR, (a) orbit 1382, day 274; (b) orbit 1339, day 271.

7.2. Ice-Motion

The initial demonstration of sea-ice drift measurement is graphical. Ice features, in particular ice-floes, were plotted on transparent paper laid out over the 8 m long image strips. A number of floes were identified on sequential images.

The coast of Banks Island was used to register the plots, and a geographical grid with latitude and longitude was generated using the tick marks of the image of revolution 1038. Only one grid was plotted since grids from different strips were inconsistent due to erroneous tick-marks.

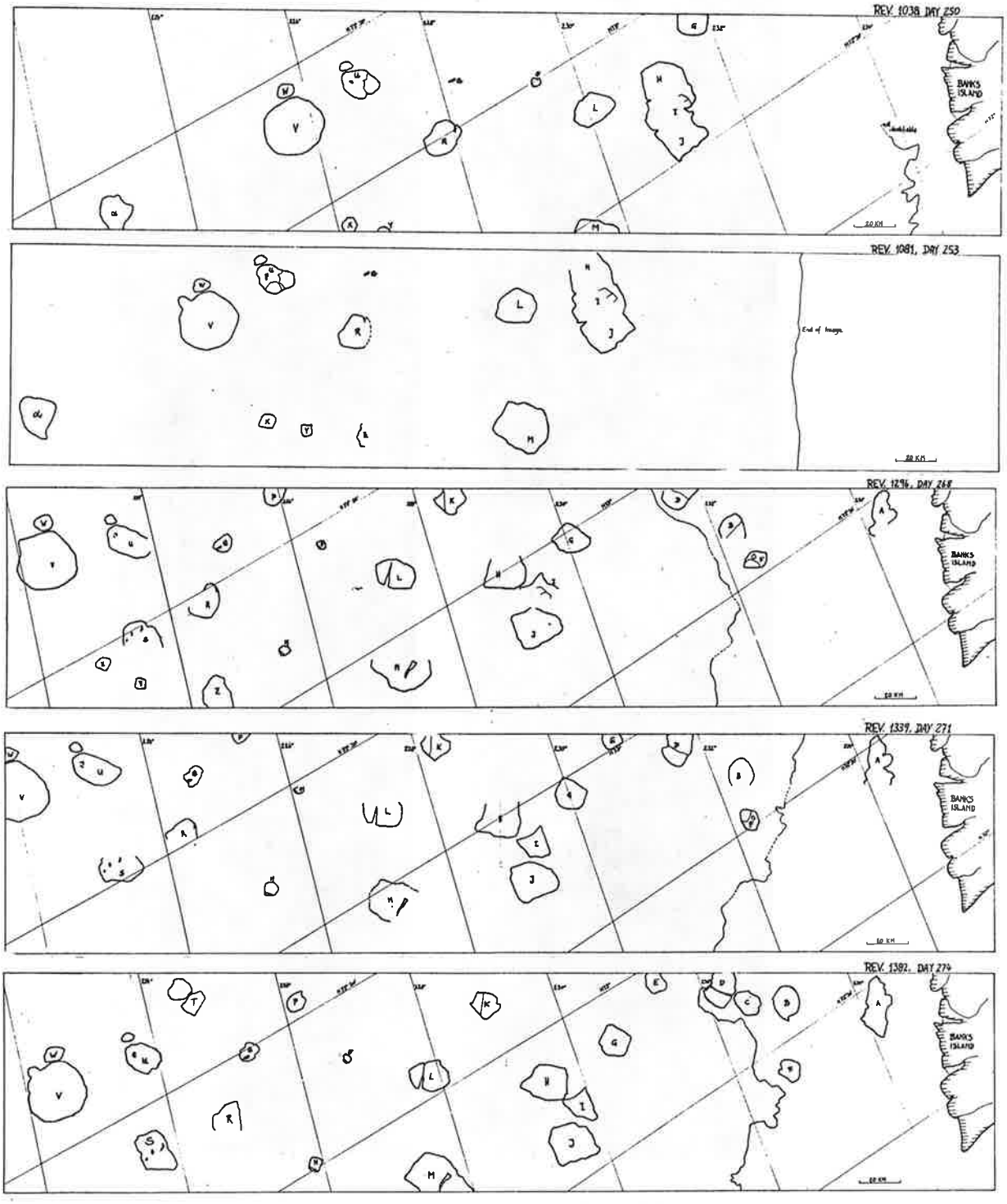

Figure 14: Plots of selected ice-floes illustrating motion of sea-ice. Plots were generated from optical correlated Seasat-SAR images. Geographical grid is derived from time-marks on orbit 1296 and is appr. only.

Figure 14 presents the five plots of ice-floes. Clearly one can observe the motion of the ice in the amount of 110 km over a period of 24 days (day 250 through 274 of 1978). While there was no problem in identifying the same ice-flow on two or three sequential features, this is very difficult over the entire 24-day-period. It is much easier to identify point-like features. There is a multitude to be recognized on all five images -- the floes themselves, however, tend to break up and change shapes so that only a very few can be observed on all passes.

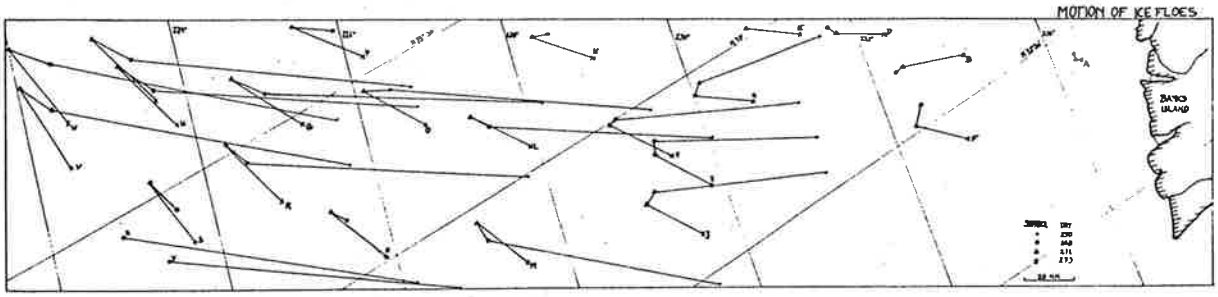

Figure 15: Presentation of motion of individual ice-floes on results from Figure 14.

Figure 15 summarizes the motion of the individual ice-floes for all passes. The strip from day 253 could not be incorperated since both Bank Island and tick marks are missing on that strip. Figure 11 demonstrates irregular ice-drift that is particularly chaotic near the shore of Banks Island.

8. CONCLUSION, OUTLOOK

Seasat-SAR images permit one to locate points on the ground with respect to ground control with an accuracy of ± 100 to ± 200 m. The greatest difficulty derives from precise identification. Good points can be identified with errors of ± 50 to 200 m.

Differences between optically and digitally correlated SAR-images are in resolution and ease of orienting oneself in the image. Once a point can be identified in the image, its accuracy is not distinctly higher on the digital as compared to the optical image.

Absolute accuracy, evaluated using no ground control but only tick-marks and Seasat orbit data, amounts to m in the image that was available. Sea-ice drift can be measured from Seasat-SAR images. Ice floes are difficult to identify over a series of more than 3 images taken sequentially. Individual ice features, such as a characteristic set of ridges on the ice, can be conveniently identified over all images. Observed ice motion amounted to about 110 km over the period of 24 days.

Seasat terminated its operation 3 month after launch. This did not permit to eliminate certain flaws in the data processing system, and it prevented

an interest to grow worldwide in Seasat-SAR data. Landsat, when launched in 1972 with its first satellite, had more time available to get data processing systems properly tuned and, over the years had generated tremendous scientific interest that has been denied to Seasat.

Satellite radar imaging will be carried on. The next such mission will be on board of the Space Shuttle, in its second launch(operational flight test 2, OFT-2) . This Space Shuttle Imaging Radar (SIR - A) mission will work with the same type of radar as Seasat, but at look angles that are less steep and somewhat more amenable to land applications. After all -- Seasat-SAR was designed for ocean observation and not for land.

ACHNOWLEDGMENT

Dr. Bill Campbell of the US Geological Survey is responsible for ice dynamics studies with Seasat-SAR images.To him and to Dr. Charles Elachi of the Jet Propulsion Laboratory, I owe many thanks for providing me sponsorship to do this ongoing effort.

REFERENCES

HARGER R.O. (1970): "Synthetic Aperture Radar Systems", Academic Press, New-York.

KRATKY V. (1979): "Effects of Seasat Orbiting on Imaging Geometry of Synthetic Aperture Radar." 3rd Intl. GOTA-Conference on Cartographic Processing and Analysis of Satellite Imagery, Toulouse, 19. - 22. June.

LEBERL F. (1978 a): "Satellitenradargrammetrie," Deutsche Geodätische Kommission, Reihe C, Nr. 238, Munich.

LEBERL F. (1978 b): "Zur Herstellung von Karten mittels Satellitenphotographie und Fernerkundungsverfahren", Geowissenschaftliche Mitteilungen, der Techn. Univ. Wien, Vol. B., pp 189 - 224.

LEBERL F. (1976) : "Imaging Radar Applications to Mapping and Charting", Photogrammetria, Vol. 32, pp 75 - 100.

LEBERL F. (1975) : "Photogrammetric Interpolation", Photogrammetric Engineering, pp 603 - 612.

PHILLIPS R. et al. (1973): "Apollo Lunar Sounder Experiment," Apollo Preliminary Science Report, NASA-Special Report 330, Washington D.C., U.S.A.

TELEKI P., RAMSEIER R. (1978): "The Seasat- A Synthetic Aperture Radar Experiment" Proceedings, Intl. Symp. , Intl. Soc. for Photogrammetry, Comm. IV, July 2- 8, Freiburg, FRG, Volume 1, pp 93 - 114.